J. Cent. South Univ. (2015) 22: 4097−4104
DOI: 10.1007/s11771-015-2955-2

Springer

Preparation and characterization of ultrananocrystalline diamond films in H_2/Ar/CH_4 gas mixtures system with novel filament structure

FENG Jie(丰杰)[1, 2], LI Sha-sha(李莎莎)[1], LUO Hao(罗浩)[1], WEI Qiu-ping(魏秋平)[1, 3], WANG Bing(王兵)[4],
LI Jian-guo(李建国)[2], HU Dong-ping(胡东平)[2], MEI Jun(梅军)[2], YU Zhi-ming(余志明)[1, 3]

1. School of Materials Science and Engineering, Central South University, Changsha 410083, China;
2. Institute of Systems Engineering, China Academy of Engineering Physics, Mianyang 621900, China;
3. State Key Laboratory of Powder Metallurgy (Central South University), Changsha 410083, China;
4. School of Materials Science and Engineering, Southwest University of Science and Technology,
Mianyang 621010, China

Abstract: Diamond films were prepared by hot filament chemical vapor deposition (HFCVD) in a gas mixtures system of methane, argon and hydrogen. The composition and morphology in different deposition pressures and filament structures were investigated, as well as the friction and wear-resistant properties. The sp^3-bonded content was measured and nano-mechanics properties were also tested. Results of atomic force microscopy and X-ray photoelectron spectroscopy show that the diamond films whose surface roughness is less than 10 nm and sp^3-bonded content is greater than 70% can be prepared by bistratal filament structure with optimized proportion of Ar. It is also shown that the friction coefficient of diamond films is 0.13 and its wear-resistant property is excellent. Nano-mechanics of films shows that its elastic modulus is up to 650 MPa and hardness can reach higher than 60 GPa. The diamond films with excellent performance have a broad application prospect in microelectromechanical systems (MEMS).

Key words: ultrananocrystalline diamond; hot filament chemical vapor deposition (HFCVD); nano-mechanics properties; bistratal filament structure

1 Introduction

Ultrananocrystalline diamond (UNCD) films [1] have low friction coefficient and high wear-resistant property, which can effectively reduce friction and wear, and improve the usability and reliability of microelectromechanical systems (MEMS) when being applied to the motion parts of microactuator [2−3]. Besides, nanocrystalline diamond films can be compatible with MEMS production processes after graphical reactive ion etching process. Previously, lithographic techniques were developed for the fabrication of UNCD-MEMS components, making UNCD a promising material for the development of high performance MEMS devices [4−5].

In recent years, the requirements for materials are increasing with the development of MEMS technology. However, larger surface roughness and the uncertainty of film thickness uniformity keep the ordinary microcrystalline diamond film (MCD) form being used widely among microelectronics and MEMS, making synthesis of diamond films with smooth surface an important research focus [6]. Since the early 1990s, GRUEN and his group from Argonne National Laboratory [7] have carried on the research of nanocrystalline diamond films by microwave plasma assisted chemical vapor deposition (MWCVD) and prepared high quality nanocrystalline diamond films, which has been drawn much attention. At present, many scholars have devoted to the research in this field and plenty of research results have been published [8−10].

As with MWCVD [11], HFCVD is also the commonly used and simple method to prepare diamond films, which has many advantages including suitable growth rates and better quality [12]. However, related reports on preparing nanocrystalline diamond films by HFCVD are few and the grain size obtained was greater than 20 nm [13]. In this work, ultrananocrystalline diamond films with smooth surface are prepared in a

---

Foundation item: Projects(51301211, 21271188) supported by the National Natural Science Foundation of China; Project(ZZ13005) supported by the Foundation of Laboratory of Ultra Precision Manufacturing Technology of China Academy of Engineering Physics; Project(2010A0302013) supported by Research Foundation of China Academy of Engineering Physics; Project(2012M521541) supported by the China Postdoctoral Science Foundation; Project(20110933K) supported by the State Key Laboratory of Powder Metallurgy (Central South University), China; Project(CSU2013016) supported by the Open-End Fund for Valuable and Precision Instruments of Central South University, China
Received date: 2014−10−20; **Accepted date:** 2015−05−05

Corresponding author: YU Zhi-ming, Professor; Tel: +86−731−88830335; E-mail: zhiming@csu.edu.cn

system with methane, argon and hydrogen as source gas by the improved HFCVD processing. Effects of gas composition, deposition pressure, substrate temperature, filament structures and heating methods are investigated. In order to increase the secondary nucleation rate and achieve the purpose of the preparation of nanocrystalline diamond films, several methods including negative bias enhancement, optimized pretreatment and deposition parameters are investigated in a combined or separate manner. This work will lay the foundation for the application of ultrananocrystalline diamond films in MEMS.

2 Experimental details

2.1 Deposition devices

Diamond films were prepared by self-developed bell-jar HFCVD device which consists of four parts: vacuum reaction chamber, valve system, measurement system and heating system, as shown in Fig. 1.

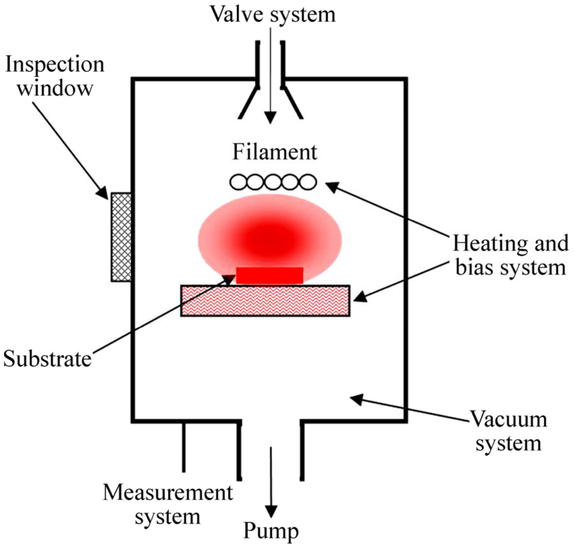

Fig. 1 HFCVD system diagram

In the HFCVD reactor, there are filaments of tungsten (W), which are heated up to 2000−2200 °C, and CH_4 and H_2 molecules that have touched the hot filament are thermally dissociated to be fragmented hydrocarbons and atomic hydrogen. They diffuse onto the substrate to create diamonds. An advantage of hot filament CVD reactors over MPCVD reactors is the simplicity of the system and a uniform diamond deposition over such a large area as 40 cm×60 cm. The HFCVD method possesses the ability to adjust to a wide variety of carbon gas sources such as methane, propane, ethane, and other hydrocarbons. Even oxygen-containing hydrocarbons including acetone, ethanol, and methanol can be used.

With the aim of improving the phase purity and growth rate of diamond, some modifications have been incorporated into the typical design of HFCVD. In the experiments, the single filament structure heating system has been modified into bistratal filament structure so that the device would further improve the plasma ionization rate of the gas and increase the nucleation rate of the film. More activated hydrogen atom and carbon species would be produced and adsorbed on the substrate after the dissolution of the gas on the filament surface, resulting in very fine and uniform diamond particulates. At the same time, bias loading method is more flexible by the process modification, thus both filament temperature and plasma kinetic energy are increased. Therefore, high secondary nucleation rate can be maintained over the preparation, and ultrananocrystalline diamond films can be obtained. The details of the heating and bias system are shown in Fig. 2.

During the deposition, the temperature of substrate and filament was monitored using single-wavelength infrared thermometer.

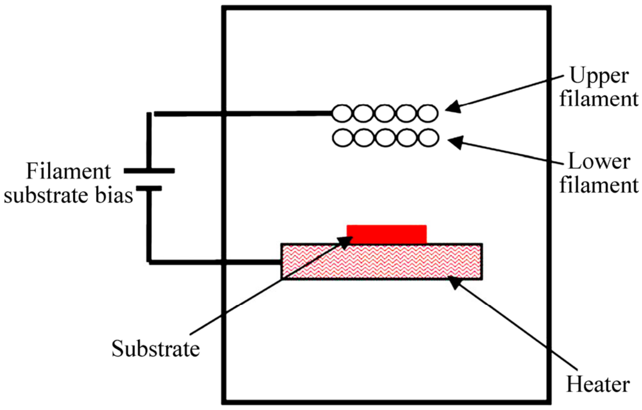

Fig. 2 Filament, substrate and power system connection diagram

2.2 Process conditions

The Si substrate (the polished slices of p-type doped Si(100) with a thickness of 0.5 mm) was pre-treated by scratching with diamond micro-powders and ultrasonic abrasion in diamond powder suspension in order to enhance the nucleation of diamond films. The pre-treatment process is divided into several parts as follows: (1) The diamond powder (0.5−1.0 μm) was placed on a glass plate and grind with the polished silicon substrate until the substrate changes color; (2) The Si substrate was treated by ultrasonic abrasion in alcohol slurry of diamond powder (with average diameter of 40 μm) for 30 min; (3) The Si substrate was cleaned by ultrasonic washer in acetone, and then put into reaction chamber to deposit with diamond film after it was dried by hot air.

Experiment parameters were designed after the evaluation of results generated from the conventional HFCVD method with methane and hydrogen as source gas. We tend to focus on the variation effect of working pressure and the proportion of Ar. Moreover, the difference of single and bistratal filament was studied.

The details of deposition conditions are given in Table 1.

Table 1 A summary of various growth conditions for films to be discussed

Sample		Flow rate/(mL·min^{-1})			Pressure/kPa
		CH_4	H_2	Ar	
Single filament	S1	4	96	0	1.5
	S2	4	96	0	2.0
	S3	4	46	50	2.0
	S4	4	16	80	2.0
	S5	4	6	90	2.0
	S6	4	0	96	2.0
	S7	4	46	50	3.0
	S8	4	96	0	4.0
	S9	4	46	50	4.0
Bistratal filament	B1	4	96	0	1.5
	B2	4	16	80	1.5
	B3	4	46	50	1.5
	B4	4	96	0	2.0
	B5	4	46	50	2.0
	B6 (polishing)	4	46	50	2.0
	B7	4	16	80	2.0
	B8	4	96	0	4.0

Distance: 6−8 mm; Substrate temperature: 880−950 °C; Growth time: 5−6 h.

2.3 Micro-analysis characterization

In this work, ESCALAB250 tape using monochromatic Al K_α X-ray source (1486.6 eV) X-ray photoelectron spectroscopy (XPS) was used to measure the ratio of sp^3-bonded and sp^2-bonded contents of the diamond films. The beam spot size of X-ray source is 500 μm.

The Almega XR laser Raman spectrometer (Thermo Nicolet Corporation) was used to analyze the state of carbon bonding. And the wavelength of excitation laser is 532 nm.

The three-dimensional morphology and two-dimensional projection of film surface were observed by atomic force microscope (AFM) which was utilized to determine surface roughness and grain size of films.

2.4 Friction−wear properties testing

Friction and wear properties of films were tested by the UMT-2M friction−wear tester of CETR Corporation. This tester works by the method of reciprocating motion with ball-on-disk. The concrete testing parameters are as follows: unlubrication friction under atmospheric conditions, room temperature (24 °C), load 2 N, reciprocating frequency 240 times/min, grinding defect length 10 mm, and testing time 30 min. The wear parts of this testing is Si_3N_4 ceramic ball (GB 308—89) and its diameter is 6.35 mm. The abrasion loss is the wear depth under specified testing conditions, tested by 2201 surface roughmeter.

2.5 Nano-mechanics properties testing

In this work, MTS nano indenter DCM testing and diamond Berkovich indenter were used to measure nanomechanical property of film and concrete parameters included load resolution of 1 nN and displacement resolution of 0.0002 nm. The changing values of hardness and modulus with pressed depth were chosen to control the parameters (constant strain rate 0.05 s^{-1}, thermal drift rate <0.05 nm/s, and constant pressed depth 1000 nm).

3 Results and analysis

3.1 Composition of diamond films

Figure 3 shows the Raman spectra of samples deposited with different Ar proportion. Generally, the

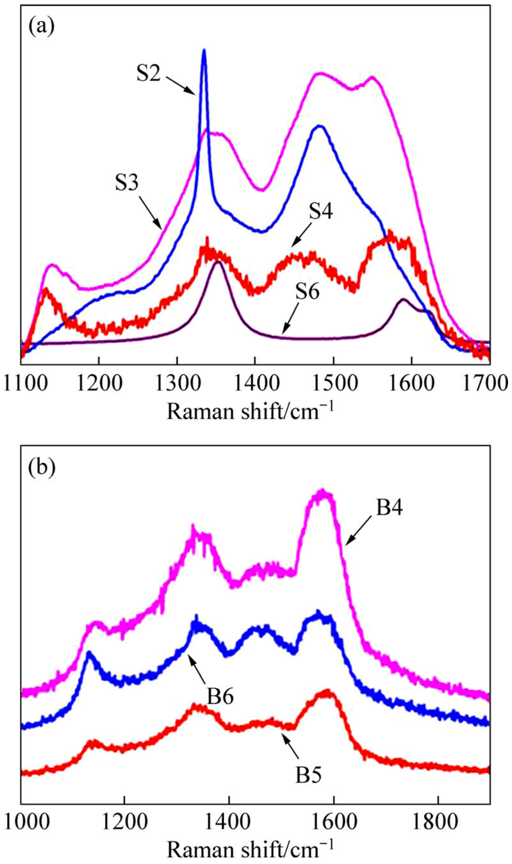

Fig. 3 Raman spectra of diamond films: (a) In single filament; (b) In bistratal

sharp Raman peak of diamond is at 1332 cm^{-1} and its scattering efficiency is only about 1/50 of the characteristic peak of graphite [14]. Therefore, Raman scattering has a higher sensitivity for graphite than diamond and can detect graphite phase from diamond films easily [15]. The graphite peak at 1580 cm^{-1} (G peak) will shift toward 1600 cm^{-1} with the decrease of grain size, and microcrystal graphite will produce peak (D peak) at 1360 cm^{-1} [16]. Amorphous carbon has two broad peaks at 1355 cm^{-1} and 1550 cm^{-1} [17]. For the hydrogenated amorphous carbon, the broad peak at 1355 cm^{-1} will become a shoulder peak of the broad peak at 1550 cm^{-1}. DLC diffusion scattering peak is situated roughly at 1480 cm^{-1}. For nanocrystalline diamond films, the characteristic peak height of diamond is very low but the full width at half maximum is very large, and the characteristic peak of diamond cannot even be observed sometimes. However, the scattering strength of non-diamond carbon structures (graphite and DLC) is very high, and there will be a scattering peak near the 1140 cm^{-1} and a new scattering peak near 1450 cm^{-1} with the advent of former peak as characteristic peaks of nanocrystalline diamond [18].

Recently, there was a further discussion about these two peaks. The result showed that the positions of two peaks vary with the change of excitation photon energy and the scattering intensity decreases as the incident photon energy increases [19]. All of these reflect the characteristic of typical sp^2-bonded hybridization. Such considerations, therefore, led FERRARI and ROBERTSON [20] to attribute both the two peaks to the C — C stretching and torsional mode of trans-polyacetylene. As shown in Fig. 3(a), the sample S2 made in the atmosphere without Ar has primarily the diamond peak at 1332 cm^{-1} and the DLC peak at 1480 cm^{-1}, indicating that the sample is composed of relatively larger micron diamond particles. On the contrary, in the sample S6 made in the atmosphere without H$_2$ and 100% Ar, only the D peak (at 1355 cm^{-1}) and G peak (at 1580 cm^{-1}) appear. In other words, there is only the graphite phase. For the sample S3 of 50% Ar, as well as the sample S4 of 80% Ar, there are a broad peak at 1332 cm^{-1} superimposed on the broad peak at 1355 cm^{-1} and other two broad peaks at 1480 cm^{-1} and 1580 cm^{-1}. It is shown that both these two films contain three carbon phases (diamond, amorphous carbon and graphite). Considering the minute difference between the peak intensity at 1580 cm^{-1} and 1332 cm^{-1} (diamond peak) and the scattering efficiency factor of two peaks, a conclusion can be drawn that graphite content in the film is far less than diamond content. These two samples both have nanocrystalline diamond characteristic peaks at 1140 cm^{-1} and 1450 cm^{-1}, which proves that the two samples are pure and the grain is fine [21].

The Raman analysis result of films made by bistratal filament and different Ar contents is shown in Fig. 3(b). For the samples B4, B5 and B6, which were made in atmosphere with different Ar contents (0%, 50% and 80% Ar), the shape and position of Raman peaks are roughly identical. Compared to the Raman peaks of single filament simples, these Raman peaks are more smooth and also include diamond peak at 1332 cm^{-1} superimposed on D peak at 1355 cm^{-1}, G peak at 1580 cm^{-1} and nanocrystalline diamond peaks at 1140 cm^{-1} and 1450 cm^{-1}. These peaks show that these films contain three carbon phases (diamond, amorphous carbon and graphite). Due to the minute difference between the peak intensity at 1580 cm^{-1} (G peak) and 1332 cm^{-1} (diamond peak), a conclusion can be drawn that graphite content in the film is far lower than diamond content, and the three films are pure and grains are fine [21].

3.2 Proportion of sp^2-bonded and sp^3-bonded content

The contents of sp^2-bonded and sp^3-bonded can be tested by the spectrum unscrambling of C 1s peak using XPS since the C 1s peak (at about 285 eV) is superposed by sp^3-bonded peak (284.2 eV) and sp^2-bonded peak (285.0 eV). The typical spectrogram of C 1s peak is shown in Fig. 4. And the sp^3-bonded content of ultrananocrystalline diamond films fabricated at different conditions is listed Table 2.

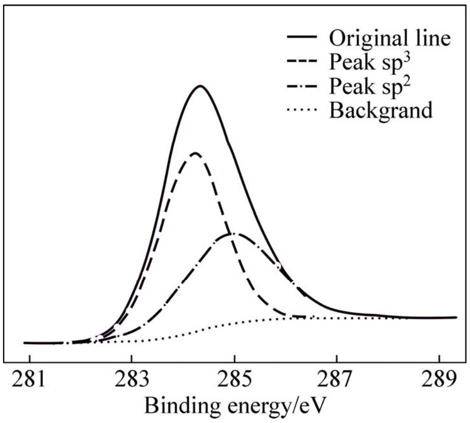

Fig. 4 Typical XPS spectrogram of C 1s peak

Table 2 sp^3 content of sp^3-bonded peak samples in different Ar proportions for S2, S3, S4, S5 and S6 samples

Sample	sp^3-bonded peak		sp^2-bonded peak		sp^3-bonded content/%
	E_b/eV	FWHM/eV	E_b/eV	FWHM/eV	
S2	284.2	0.98	285.0	1.48	77.8
S3	284.3	1.58	285.1	2.1	73.5
S4	284.4	1.64	285.2	1.91	70.2
S5	284.2	1.54	285.0	2.17	58.4
S6	284.4	1.18	285.2	1.75	53.2

According to Table 2, the sp^3-bonded contents of ultrananocrystalline diamond films (Ar content>80%, samples S2, S3 and S4) are all above 70%. The sp^3-bonded content will drop to below 60% when the proportion of Ar is set above 90% (samples S5 and S6). Although there is a certain sp^3-bonded content for samples S5 and S6, the property of films decreases clearly. As the graphite phase appears, the film becomes porous and significant shedding of powder graphite appears during the polishing process for samples. This proves that the deposition of ultrananocrystalline diamond films requires precise limitation of Ar content.

3.3 Morphology of diamond films

Figure 5 shows the SEM morphology of diamond films grown by the deposition technology of typical microcrystalline and nanocrystalline. For microcrystalline diamond, the crystal size of sample S8 is about 3−5 μm and {111} surface dominates in the sample (Fig. 5(a)). However, in sample B8, crystal size is about 2−3 μm and {100} surface dominates (Fig. 5(b)). This proves that the bistratal filament system benefits grain refinement and orientation growth. For nanocrystalline diamond, nanoparticles are obvious in both S1and B1 samples (Figs. 5(c) and (d)). The surface of these films is flat and smooth. Moreover, the aggregation of diamond particles including lots of tiny grains proves that the second nucleation exists in these films.

Figure 6 shows the observed result of AFM about the films with different pressures in single filament system. According to the 3D images, the surface roughnesses of S3, S7 and S9 samples are 13.8 nm, 20.4 nm and 27.5 nm, respectively (Table 3). It is shown that grain size increases as pressure decreases. The structure of these films is very dense with fine grain size and unclear grain boundaries. There are some significantly greater aggregates in films, and then the aggregates gather into the film with the nanocrystalline. These cause the increase of film surface irregularity and roughness. The surface irregularity increases as the pressure increases, proving that some grains grow larger under the greater pressure. For the sample deposited in the atmosphere with the proportion of Ar over 90% (not shown), the graphite will be grown, however, pressure changes. The result shows that finer grains and smoother

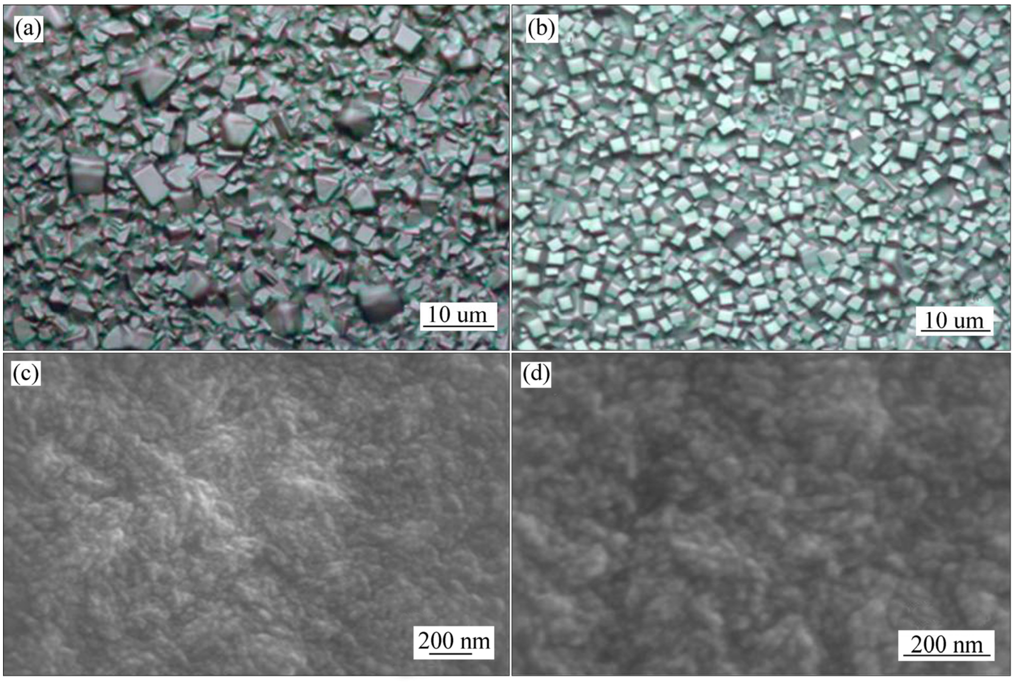

Fig. 5 SEM morphologies of microcrystalline and nanocrystalline in single and bistratal systems: (a) Sample S8; (b) Sample B8; (c) Sample S1; (d) Sample B1

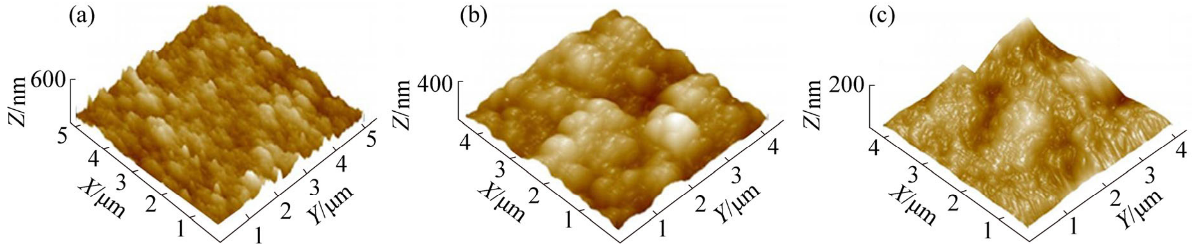

Fig. 6 AFM morphologies with different pressures in single filament system: (a) Sample S3; (b) Sample S7; (c) Sample S9

Table 3 Surface roughness of samples under different pressures in single filament system

Sample	Surface roughness, R_a/nm
B3	13.8
B7	20.4
B9	27.5

films can be obtained under lower deposition pressure in the condition of single filament.

The result of AFM of the films made in atmosphere which contains 4% CH_4 and 50% or 80% Ar with the pressure of 2 kPa or 1.5 kPa by bistratal filament is shown in Fig. 7. It can be observed that the surface roughness of films made in the atmosphere with 50% Ar reduces from 16.1 nm to 13.2 nm with the pressure decreasing from 2 kPa to 1.5 kPa (Table 4). Compared with single filament, changes in the surface roughness of films in bistratal filament are not significant, but the grain distribution is more uniform and there are no obvious aggregates. The film surface roughness drops to 9.7 nm with Ar content increasing to 80% (Table 4). The result shows that the size of diamond particulates can be further decreased by the optimization of process and the film surface degree of finishing can be improved.

Another method to improve surface finish is by polishing sample surface very gently. The morphology observed from AFM patterns of sample which endures light surface polishing is shown in Fig. 7(d). It is observed that sample surface roughness decreases to 1 nm by polishing which can meet the requirement of application in surface acoustic wave reflector device or optical film.

3.4 Surface friction properties

In order to compare friction and wear-resistant properties of diamond films with different surface roughness prepared in different systems, the surface roughness of different samples was measured by the surface roughometer before the friction testing, as listed in Table 5. The result is roughly consistent with the testing result by AFM.

Figure 8 shows the friction coefficient versus time. The test data of the wear depth and friction coefficient under the condition of this test are listed in Table 5.

It is proved that the friction coefficient of ultrananocrystalline diamond films which are fabricated by bistratal filament is less than 0.15 under certain conditions (the friction coefficient of samples fabricated by single filament is 0.6−0.7 under the same conditions), which is better than the films of single filament. Considering wear depth, it is deeper in single filament system than in bistratal filament system. It is indicated that the films of bistratal filament are more compact and the wear-resistant properties are better. Besides, the surface morphology will be affected by Ar content under the condition of bistratal filament, making friction and wear-resistant properties different among the films fabricated in different Ar contents [22]. And the friction coefficient of sample B1 is lower because the surface is smooth under this processing condition. This shows that the films have a better wear resistance and low coefficient friction, making it an ideal candidate for the production of driving part in MEMS.

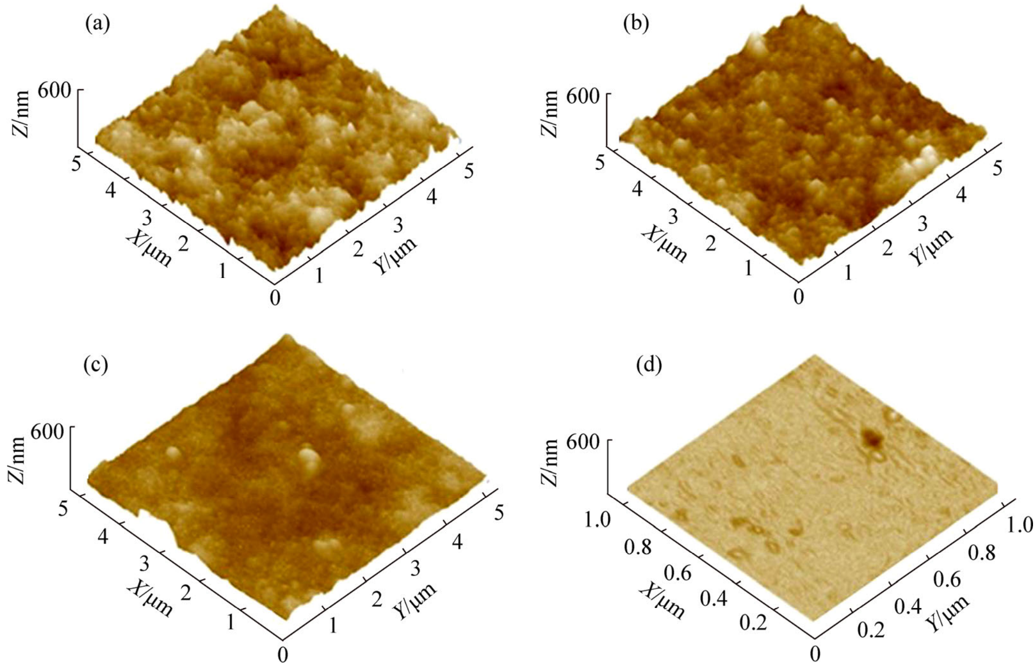

Fig. 7 AFM morphologies with different pressures in bistratal filament system: (a) Sample B5; (b) Sample B3; (c) Sample B7; (d) Sample B6

Table 4 Surface roughness of samples under different pressures in bistratal filament system

Sample	Surface roughness, R_a/nm
B5	16.2
B3	13.2
B7	9.7
B6	0.4

Table 5 Friction and wear-resistant properties of diamond films in different deposition conditions

Sample	Surface roughness, R_a/nm	Wear depth/μm	Average friction coefficient
S1	29.0	0.09	0.202
B1	12.0	0.02	0.117
B3	14.0	0.04	0.131

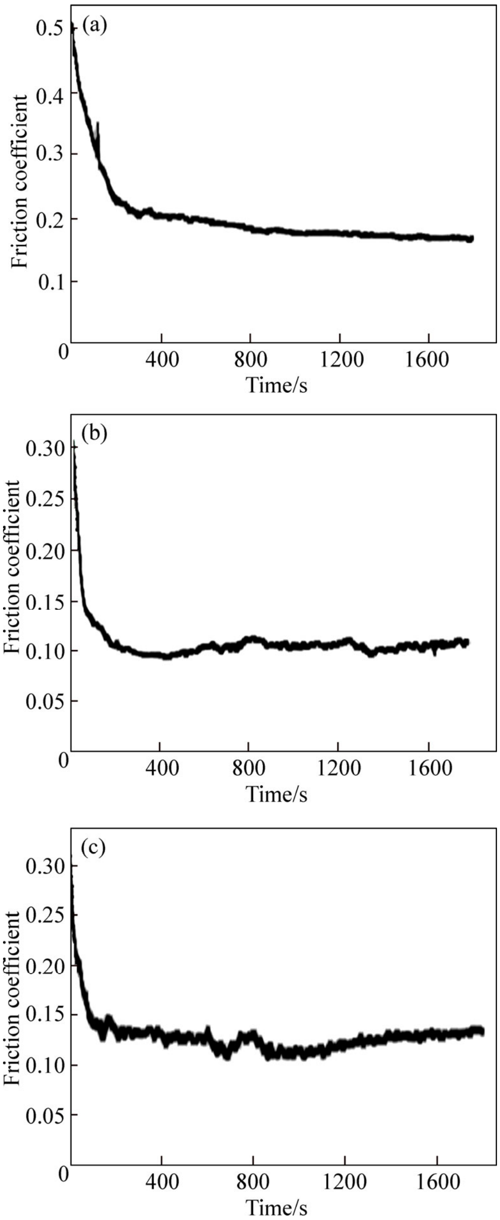

Fig. 8 Curves of friction coefficient and time in different deposition conditions: (a) Sample S1; (b) Sample B1; (c) Sample B3

3.5 Effect of atmosphere on nano-mechanics properties

The samples were prepared by bistratal filament under the pressure of 2 kPa with 4% CH_4 and different proportions of Ar. The nanohardness and modulus of films are listed in Table 6. The hardness and modulus of sample reduce significantly as the proportion of Ar increases. When the proportion of Ar exceeds 80%, the strength has been reduced to the silicon substrate level. The reason is that Ar atmosphere has a role in refining grains and generating more amorphism of sp^2-bond and graphite phase. The microscopic mechanical properties of thin films including hardness and modulus are determined by the content of sp^2-bonded and sp^3-bonded contents and the test results are roughly consistent with XPS results. However, certain differences exist between the testing result of Raman spectra and friction and wear properties, so further research is needed.

Table 6 Modulus and hardness in samples prepared with different Ar proportions

Sample	Modulus/MPa	Hardness/GPa
B4	654.8	61.4
B5	210.7	24.0
B7	67.8	10.2
Si substrate	180	12.5

4 Conclusions

1) Ultrananocrystalline diamond films can be fabricated by adjusting proportion of Ar and selecting appropriate reaction gas pressure in the system of methane, argon and hydrogen.

2) Methods used in this work can further increase secondary nucleation density and refine the grains. Surface roughness is controlled below 10 nm using the bistratal heating filament.

3) The friction coefficient of ultrananocrystalline diamond films fabricated in system of methane, argon and hydrogen can reach 0.13. So, the films have good wear-resisting property and can meet the requirement of driving part in MEMS.

References

[1] CORRIGAN T D, GRUEN D M, KRAUSS A R, ZAPOL P, CHANG R P H. The effect of nitrogen addition to Ar/CH_4 plasmas on the growth, morphology and field emission of ultrananocrystalline diamond [J]. Diamond Related Materials, 2002, 11(1): 43−48.

[2] SUMANT A V, AUCIELLO O, LIAO M. MEMS/NEMS based on mono-, nano-, and ultrananocrystalline diamond films [J]. Mrs Bulletin, 2014, 39(6): 511−516.

[3] SUMANT A V, AUCIELLO O, CARPICK R W. Ultrananocrystalline and nanocrystalline diamond thin films for MEMS/NEMS

applications [J]. Mrs Bulletin, 2010, 35(4): 281−288.

[4] AUCIELLO O, SUMANT A V. Status review of the science and technology of ultrananocrystalline diamond (UNCD™) films and application to multifunctional devices [J]. Diamond Related Materials, 2010, 19: 699−718.

[5] KRAUSS A R, AUCIELLO O, GRUEN D M, JAYATISSA A, SUMANT A, TUCEK J, MANCINI D C, MOLDOVAN N, ERDEMIR A, ERSOY D, GARDOS M N, BUSMANN H G, MEYER E M, DING M Q. Ultrananocrystalline diamond thin films for MEMS and moving mechanical assembly devices [J]. Diamond Related Materials, 2001, 10: 1952−1961.

[6] MICHALAS L, SAADA S, KOUTSOURELI M. Reliability of nanocrystalline diamond MEMS capacitive switches [C]// 8th European Microwave Integrated Circuits Conference (Eumic). Nuremberg, Germany: IEEE, 2013: 364−367.

[7] GRUEN D M. Nanocrystalline diamond films [J]. Annual Review of Materials Science, 1999, 29: 211−259.

[8] MAY P W, SMITH J A, MANKELEVICH Y A. Deposition of NCD films using hot filament CVD and $Ar/CH_4/H_2$ gas mixtures [J]. Diamond Related Materials, 2006, 15(2/3): 345−352.

[9] HUANG S M, HONG F C N. Low temperature growths of nanocrystalline diamond films by plasma-assisted hot filament chemical vapor deposition [J]. Surface and Coatings Technology, 2006, 200(10): 3160−3165.

[10] WANG T, XIN H W, ZHANG Z M, DAI Y B, SHEN H S. The fabrication of nanocrystalline diamond films using hot filament CVD [J]. Diamond Related Materials, 2004, 13: 6−13.

[11] ZOU Y S, LI Z X, WU Y F. Deposition and characterization of smooth ultra-nanocrystalline diamond film in $CH_4/H_2/Ar$ by microwave plasma chemical vapor deposition [J]. Vacuum, 2010, 84: 1347−1352.

[12] VAMIN V P, LAPTEV V A, RALVCHENKO V G. The state of the art in the growth of diamond crystals and films [J]. Inorganic Materials, 2006, 42: S1−S18.

[13] LIAO M Y, MENG X M, ZHOU X T, HU J Q, WANG Z G. Nanodiamond formation by hot-filament chemical vapor deposition on carbon ions bombarded Si [J]. Journal of Crystal Growth, 2002, 236: 85−89.

[14] SUN Bi-wu, ZHAGN Xiao-pin, LIN Zhang-da. Growth mechanism and the order of appearance of diamond (111) and (100) facets [J]. Physical Review B, 1993, 47(15): 9816−9824.

[15] SANKARAN K J, PANDA K, SUNDARAVEL B. Enhancing electrical conductivity and electron field emission properties of ultrananocrystalline diamond films by copper ion implantation and annealing [J]. Journal of Applied Physics, 2014, 115(6): 063701.

[16] CEBIK J, MCDONOUGH J K, PEERALLY F. Raman spectroscopy study of the nanodiamond-to-carbon onion transformation [J]. Nanotechnology, 2013, 24(20): 205703.

[17] FERRARI A C, ROBERTSON J. Interpretation of Raman spectra of disordered and amorphous carbon [J]. Physical Review B, 2000, 61: 14095.

[18] NEMANICH R, GLASS J, LUCOVSKY G, SHRODER R. Raman scattering characterization of carbon bonding in diamond and diamondlike thin films [J]. Journal of Vacuum Science & Technology A, 1988, 6: 1783−1787.

[19] CHEN S T, CHU Y C, LIU C Y. Surface-enhanced Raman spectroscopy for characterization of nanodiamond seeded substrates and ultrananocrystalline diamond at the early-stage of plasma CVD growth process [J]. Diamond and Related Materials, 2012, 24: 161−166.

[20] FERRARI A C, ROBERTSON J. Origin of the 1150-cm^{-1} Raman mode in nanocrystalline diamond [J]. Physical Review B, 2001, 63: 121405.

[21] CORRIGAN T, GRUEN D, KRAUSS A, ZAPOL P, CHANG R. The effect of nitrogen addition to Ar/CH_4 plasmas on the growth, morphology and field emission of ultrananocrystalline diamond [J]. Diamond Related Materals, 2002, 11: 43−48.

[22] LIANG Xing-bo, WANG Lei, ZHU Hong-liang, YANG De-ren. Effect of pressure on nanocrystalline diamond films deposition by hot filament CVD technique from $CH_4/H_2/Ar$ gas mixture [J]. Surface & Coating Technology, 2007, 202: 261−267.

(Edited by YANG Bing)